Pulse Splitting in Short Wavelength Seeded Free Electron Lasers

M. Labat,[1,*] N. Joly,[2,3] S. Bielawski,[2] C. Szwaj,[2] C. Bruni,[4] and M. E. Couprie[1]

[1]*Synchrotron SOLEIL, Saint Aubin, BP 34, 91 192 Gif-sur-Yvette, France*

[2]*Laboratoire des Physique des Lasers, Atomes et Molécules, UMR CNRS 8523, Centre d'Études et de Recherches Lasers et Applications, FR CNRS 2416, Université des Sciences et Technologies de Lille, F-59655 Villeneuve d'Asq Cedex, France*

[3]*University of Erlangen-Nuremberg, Guenther-Scharowsky Strasse 1/bau 24, 91058 Erlangen, Germany*

[4]*LAL, Université Paris-Sud 11, UMR 8607, batiment 200, 91898 Orsay Cedex, France*

(Received 24 September 2009; published 23 December 2009)

We investigate a fundamental limitation occurring in vacuum ultraviolet and extreme ultraviolet seeded free electron lasers (FELs). For a given electron beam and undulator configuration, an increase of the FEL output energy at saturation can be obtained via an increase of the seed pulse duration. We put in evidence a complex spatiotemporal deformation of the amplified pulse, leading ultimately to a pulse splitting effect. Numerical studies of the Colson–Bonifacio FEL equations reveal that slippage length and seed laser pulse wings are core ingredients of the dynamics.

DOI: 10.1103/PhysRevLett.103.264801 PACS numbers: 41.60.Cr, 42.65.Ky

Short duration, short wavelength, and high power electromagnetic radiation enables the investigation of ultrafast phenomena at the atomic scale. Nowadays, x-ray sources can be provided by synchrotron light sources [1], harmonic generation in gas [2], and on solid targets [3,4] or Thomson scattering [5], for example. One of the most powerful and promising devices is the single pass free electron laser (FEL) [6,7]. In a FEL system, a relativistic electron beam wiggles on an oscillating trajectory forced by the periodic magnetic field of an undulator, and interacts with optical radiation which can be provided either by the electron beam spontaneous emission [6] or a coherent external source [8] referred as a seed. The seeded FEL offers the highest temporal coherence. In such a system, the dynamical regime determines output radiation pulse characteristics [9]. For instance, in the steady-state regime, the FEL power saturates after scaling as $z^{4/3}$, with z the distance in the undulator, while in the superradiant regime [10–12], the FEL power does not saturate and scales as z^2.

In this Letter, we theoretically evidence a new spatiotemporal regime, for which the emitted FEL pulse splits into two subpulses. This dynamical behavior occurs in seeded FEL with long seed pulse duration and may be relevant for the next generation short wavelength seeded FELs such as ARC-EN-CIEL [13], FERMI [14], and SPARX [15]. The understanding and control of these regimes is essential for the optimization of the FEL sources in terms of output power and optical quality since both are demanded by users communities. Using the Colson-Bonifacio model [6,16], we evidence the behaviors of the seeded FEL and provide further insight on the pulse splitted regime, which is interpreted in terms of gain saturation.

The radiation amplification mechanism in FELs is commonly analyzed in three steps [7]: energy modulation (also referred as lethargy [6]), exponential growth, and saturation. During the first evolution step, i.e., along the first periods of the undulator, energy exchange is performed between the electrons and the radiation, leading to an energy modulation and further to a density modulation (microbunching) of the electrons at the resonant wavelength $\lambda_R = \frac{\lambda_0}{2\gamma^2}(1 + K^2/2)$. λ_R is fixed by the electron beam normalized energy γ and the undulator period λ_0 and deflection parameter K. The seed wavelength should be adjusted to λ_R. Microbunching induces coherent emission of the electron beam. In addition, the use of a coherent seed to initiate the process enables us to lock in phase the microbunches and therefore to achieve a much better temporal coherence. The FEL then enters into the second evolution step: radiation amplitude increases exponentially to the detriment of the electron beam kinetic energy. The strong energy losses, corresponding to a redshift of the resonant wavelength λ_R, end up disabling the electron-optical field interaction. In the steady-state approximation, the FEL reaches a maximum power and saturates. Its final characteristics (power, duration, spectral width) only depend on the undulator field and electron beam properties. Taking time into account, i.e., considering the beams propagation velocity, makes the FEL dynamics more complex. Since the electron wiggles at a relativistic velocity $v_z < c$, the optical pulse slips forward with respect to the electron bunch by one wavelength λ per undulator period (see Fig. 1), resulting in the so-called slippage defined as

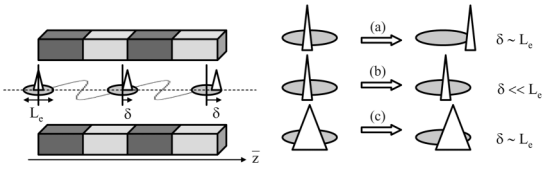

FIG. 1. Schematic of the seeded FEL initial parameters. $\bar{z}$ is the longitudinal coordinate along the undulator. L_e is the electron bunch length and δ the slippage.

$\delta = N\lambda$, i.e., the displacement of the optical pulse with respect to the electron beam at the end of the N periods of the undulator. The present quest of compact and short wavelength devices tends to reduce it. The possible slippage configurations are represented schematically in Fig. 1. In (a), a short seed pulse with respect to the bunch length is injected and slips within the undulator distance over the whole electron bunch. In (b), the slippage is shorter than the electron bunch length, which limits the interaction region. This is the operating area of several existing FELs, such as SCSS test accelerator [17], SPARC [18,19], and sFLASH [20]. We will see that using a longer seed pulse [case (c)] enables us to increase the interaction region but also eventually leads to complex spatiotemporal deformation of the optical pulse such as pulse splitting.

In universal scaling [9], the FEL dynamics can be described by the one-dimensional Colson-Bonifacio [6,16] model:

$$\frac{\partial \phi_j}{\partial \bar{z}} = p_j, \tag{1a}$$

$$\frac{\partial p_j}{\partial \bar{z}} = -[A(\bar{z},\tau)e^{i\phi j} + \text{c.c.}], \tag{1b}$$

$$\left(\frac{\partial}{\partial \bar{z}} + \frac{\partial}{\partial \tau}\right) A(\bar{z},\tau) = \chi(\tau) b(\bar{z},\tau). \tag{1c}$$

Each particle j, $j = 1 \ldots N_e$ with N_e the total number of electrons, in the optical field A, is followed in the phase space using ϕ_j, the particle relative phase, and p_j, the particle relative energy both normalized to the reference particle. The variables ϕ_j, p_j, and A are functions of the longitudinal coordinates τ along the electron bunch and $\bar{z}$ along the undulator. τ is defined within $0 < \tau < L_e$, with L_e the electron bunch length, and $\bar{z}$ is defined within $0 < \bar{z} < L_u$, with L_u the undulator length. All dimensions are in cooperation length [10,21] units: $l_c = \frac{\lambda}{4\pi\rho}$, with ρ the Pierce fundamental scaling parameter [6] characterizing the gain of the FEL. χ is the macroscopic electronic density normalized to 1 and $b(\bar{z},\tau)$ is the bunching coefficient: $b(\bar{z},\tau) = 1/N_e \sum e^{-i\phi_j}$. Equations (1a) and (1b) describe the particle dynamics while Eq. (1c) includes the pulse propagation.

The initial conditions required for the various regimes can be defined more precisely using S_e comparing the slippage length to the electron bunch length, and S_{seed} comparing the slippage length to the seed pulse duration. In the scaled units, with L_{seed} the seed pulse duration, the slippage length corresponds to the final $\bar{z} = 4\pi\rho N$, so that

$$S_e = \frac{4\pi\rho N}{L_e} \quad \text{and} \quad S_{\text{seed}} = \frac{4\pi\rho N}{L_{\text{seed}}}. \tag{2}$$

In the short electron bunch limit, i.e., $S_e \gg 1$, the FEL evolves in the weak superradiant regime [10]: the strong slippage enables the development of a narrow spike in the leading edge of the electron bunch which rapidly escapes of the electron bunch. Because of the limited interaction time, the final output power remains lower than the saturation power defined in the steady-state approximation. In the present seeded FEL context, S_e tends to decrease via the reduction of λ_R for the short wavelength operation and of N for the shortening of the undulators. SPARC [18] ($S_e \approx 0.2$) and SCSS test accelerator [17] ($S_e \approx 0.3$) seeded FELs already fall in the $S_e < 1$ area, illustrated in Figs. 1(b) and 1(c).

The FEL evolution is simulated with Eq. (1) in the long electron bunch limit, i.e., $S_e \approx 1$, for various S_{seed} values. The dynamics of the FEL pulse is illustrated in Fig. 2 using 2D diagrams with the longitudinal coordinate along the

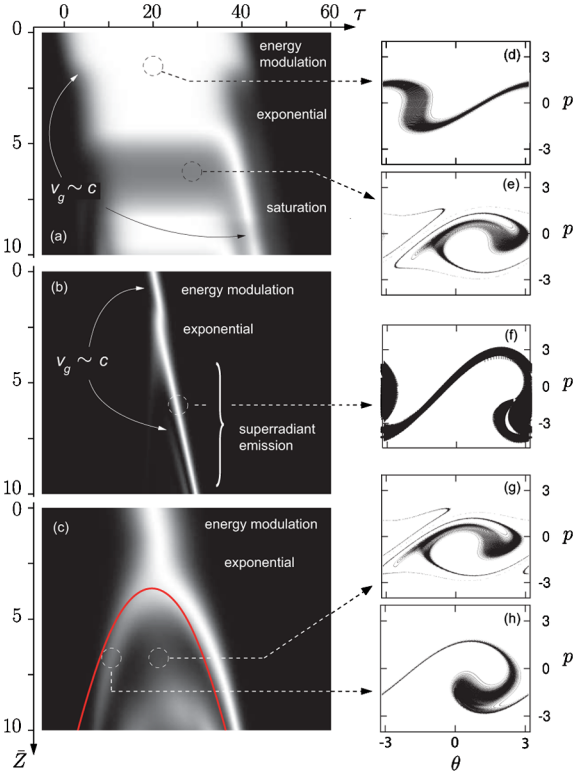

FIG. 2 (color online). Evolution of the FEL longitudinal normalized optical field intensity $|A|^2(\tau)$ along the undulator according to Eq. (1). Seed parameters: (a) $S_{\text{seed}} = 0.25$ (with hyper-Gaussian shape, $\sigma_{\text{seed}} = 40$), (b) $S_{\text{seed}} = 10$ (with Gaussian shape, $\sigma_{\text{seed}} = 1$), and (c) $S_{\text{seed}} = 2$ (with Gaussian shape, $\sigma_{\text{seed}} = 5$), (continuous line) calculation of $\bar{z}_{\text{sat}}$ according to Eq. (5). (d)–(h) Phase space of the electron beam at locations indicated on (a)–(c). Maximum seed field amplitude at $\bar{z} = 0$: $A_0 = 0.15$. Electron bunch discretized along the τ axis. Phase space consisting of 200×200 particles associated to each τ coordinate. Initially: θ_j uniformly distributed within $[-\pi, +\pi]$ and p_j following a normal distribution centered around zero with standard deviation 0.2%-RMS. Electron beam profile: flat top using super Gaussian of parameter $m = 4$ and $L_e = 40$, corresponding to $S_e = 0.25$.

electron bunch τ in the horizontal axis and the coordinate along the undulator $\bar{z}$ in the vertical axis. Figure 2(a), with $S_{\text{seed}} < 1$, represents the standard evolution of the seeded FEL which can be also obtained in the steady-state model [9]. The seed electric field first performs energy modulation of the electron bunch and slips along the electron bunch at a speed v_g close to the light velocity. Along the undulator, the energy modulation is converted into a density modulation and the particles rotate in the phase space [see Fig. 2(d)]. The optical field is then exponentially amplified to the detriment of the particles kinetic energy and slows down by the electronic medium ($v_g < c$). At the end of the exponential growth ($\bar{z} \approx 4$), the FEL saturates and the optical pulse no longer interacts with electrons and slips ahead of the bunch at the light velocity. A typical saturated phase space is presented in Fig. 2(e). For $S_{\text{seed}} > 1$ [see Fig. 2(b)], the FEL evolves into the strong superradiant regime [10–12]. At the end of the exponential growth, the optical pulse slips as in the exponential regime ahead of the electron bunch at the light velocity but no longer saturates [see Fig. 2(f)]. Considering typical designs of compact facilities in the vuv range with $N \approx 500$ and $\lambda_R \approx 10$ nm, the range $S_{\text{seed}} > 1$ corresponds to a 1 fs seed pulse duration, which can be only achieved to the detriment of the charge [22]. In the case of Fig. 2(c), $S_{\text{seed}} \approx 1$ and the development of two subpulses at the output of the exponential growth is clearly visible. At a given position in the undulator shortly after the pulse splitting location, the particle distribution in the phase space is much strongly over modulated where the splitting occurred [Fig. 2(g)] than on the tail [Fig. 2(h)]. Since overmodulation is a signature of local saturation, the bunch slices initially under the center of the seed distribution, modulated with higher optical field, reach saturation within a shorter distance in the undulator than edges slices modulated with the lower optical power of the seed wings. This delayed arrival to saturation is responsible for the generation of two pulses on the edges. Since the electrons carry on their rotation in the phase space within the optical pulse electric field, the process repeats after one cycle: additional subpulses, still generated at the center of the distribution, appear further down in the undulator. These pulses remain at a weak intensity since most of the available electrons kinetic energy has already been transferred to the first two subpulses.

Figure 3 illustrates the evolution of the FEL power (integrated over the whole pulse) along the undulator in the three cases of Fig. 2. It confirms that whatever S_{seed}, the FEL power first exponentially increases. For (a) $S_{\text{seed}} < 1$, the FEL then reaches its maximum power and saturates. For (b) $S_{\text{seed}} > 1$, in the case of strong superradiance, the FEL does not saturate: it carries on its amplification, following a z^2 evolution [12]. Indeed, the slippage enables us to push forward the pulse into the ''fresh'' unmodulated electron bunch region which maintains the feeding of the

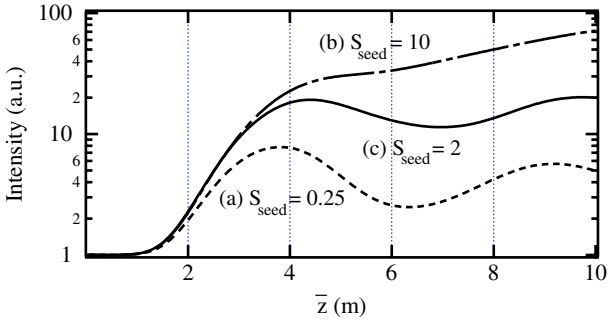

FIG. 3 (color online). Evolution of the FEL pulse intensity along the undulator calculated with Eq. (1). Intensity integrated over the whole pulse and normalized with the value at $z = 0$. (a), (b),(c) plots correspond to the (a),(b),(c) cases of Fig. 2.

pulse. Finally, in the new pulse splitting regime of case (c) $S_{\text{seed}} \approx 1$, the FEL thus with two pulses, saturates.

To investigate the origin of the pulse splitting, we study the evolution of the gain, as commonly done in conventional laser physics. Indeed, gain inhomogeneities (either spatial, polarization, or frequency hole-burning [23]) are known to be responsible for multimode emission in lasers. In the case of FELs, the gain medium consists of relativistic electrons and the gain is defined as for conventional lasers as the strength of the optical field amplification. Its expression can be derived from Eq. (1c):

$$G(\bar{z}, \tau) = \text{Re}\left[\frac{\chi(\tau) b(\bar{z}, \tau)}{A(\bar{z}, \tau)}\right]. \tag{3}$$

It is related to the bunching of the particles in the phase space. Figure 4 presents the evolution of the FEL gain along the undulator in the pulse splitting regime case of Fig. 2(b). The evolution of the gain at the center of the electron beam ($\tau = 20$) corresponds to maximum seed initial intensity. The local gain exhibits an evolution with oscillations: positive in a first step, negative around $\bar{z} \approx 4$, positive again after $\bar{z} \approx 6.5$, and finally negative at the end

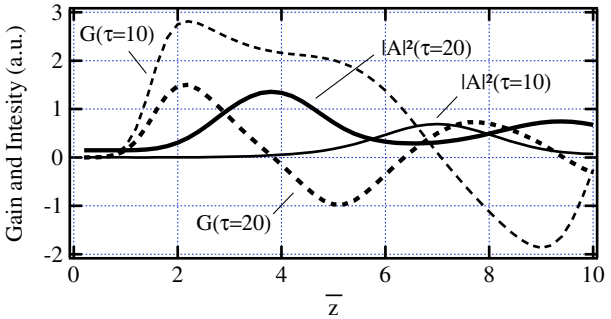

FIG. 4 (color online). Local gain and optical field intensity along the undulator. $|A|^2(\bar{z}, \tau = 10)$ line and $|A|^2(\bar{z}, \tau = 20)$ bold line calculated with Eq. (1). $G(\bar{z}, \tau = 10)$ dashed and $G(\bar{z}, \tau = 20)$ bold dashed line. Electron beam shape: gate with $L_e = 40$. $-5 < \tau < 50$. Seed shape: Gaussian with $\sigma_{\text{seed}} = 10$, $|A|(\bar{z} = 0, \tau = 20) = 0.15$, $|A|(\bar{z} = 0, \tau = 0) = 0.0025$.

of the undulator. Positive gain allows an amplification while a negative gain results in a reduction of the optical field. In addition, since the electron beam yields energy to the radiation, the oscillation amplitude of the gain decreases along the undulator. Figure 4 also presents the evolution of the gain on the tail of the electron beam ($\tau = 10$) corresponding to a lower initial seed intensity. As at $\tau = 20$, the gain oscillates with a decreasing amplitude along the undulator. Nevertheless, the oscillations are shifted in position along the undulator with respect to the $\tau = 20$ case: maximum gain is reached after a longer travel in the undulator. The analysis of Fig. 4 shows that, in the case of the pulse splitting regime, the gain saturates at a different location within the undulator depending on the longitudinal position along the electron beam, i.e., depending on the initial seed intensity. Saturation is first reached at the maximum seed intensity location. The nonuniform seed intensity profile drives inhomogeneous saturation of the gain and seems to result in pulse splitting behaviors, as in conventional laser multimode behaviors stem from inhomogeneous gain.

In the conditions of pulse splitting, $S_e < 1$ and $S_{\text{seed}} \approx 1$, the slippage $\frac{\partial A}{\partial \tau}$ can be neglected, which allows us to solve Eq. (1) in the linear approximation and to give an analytical expression of the optical field for $\bar{z} > 1$ [24]:

$$|A|^2(\bar{z}, \tau) \approx \tfrac{1}{9}\exp[\sqrt{3}\bar{z}]|A|_0^2(\tau) \tag{4}$$

with $|A|_0(\tau)$ the seeded optical field. Since the saturation is reached for $|A|^2(\bar{z}_{\text{sat}}, \tau) = O(1) \cong 1.4$ [24], the $\bar{z}_{\text{sat}}$ coordinate of the saturation as a function of the longitudinal coordinate τ along the electron bunch is derived from Eq. (4):

$$\bar{z}_{\text{sat}}(\tau) = \frac{1}{\sqrt{3}} \ln\left[\frac{9 \times 1.4}{|A|_0(\tau)^2}\right]. \tag{5}$$

Equation (5) provides a simple expression of the location and further trajectory of the subpulses along the undulator. It also reveals that the shape of the pulse splitting phenomenon can be easily controlled via seed shaping. Indeed, $\bar{z}_{\text{sat}}$ is a map of the longitudinal seed distribution $|A|_0(\tau)$. In Fig. 2(c), analytical calculation according to Eq. (5) of the pulse splitting was added (continuous line) to the full simulation and found in good agreement with it. In addition, the figure confirms that the trajectory of the subpulses can be driven by the seed shape: using even more peaked seed shape would lead to a smaller angular aperture between the two trajectories of the subpulses.

In conclusion, depending on the initial conditions (electron beam, undulator, and seed laser parameters), the seeded FEL can be driven in different evolution regimes at the end of the common exponential growth step. In the context of compact vuv seeded FELs, a new regime has been addressed in which the FEL pulse splits within two subpulses. This splitting results from the nonhomogeneous saturation of the gain by the optical field copropagating with the electron beam. While the pulse power at saturation is preserved, such a phenomenon spoils the temporal profile of the radiation. Even though pulse splitting can be avoided by increasing the gain length, further analysis is being done to suppress the entire regime and force the FEL into the superradiant regime only by monitoring the seed laser shape.

*marie.labat@synchrotron-soleil.fr

[1] E. R. Elder *et al.*, Phys. Rev. **71**, 829 (1947).
[2] M. Zepf *et al.*, Phys. Rev. Lett. **99**, 143901 (2007).
[3] B. Dromey *et al.*, Phys. Rev. Lett. **99**, 085001 (2007).
[4] R. Horlein *et al.*, Eur. Phys. J. D (to be published).
[5] K. Ta Phuoc *et al.*, Phys. Rev. Lett. **91**, 195001 (2003).
[6] B. Bonifacio *et al.*, Opt. Commun. **50**, 373 (1984).
[7] L. H. Yu, Phys. Rev. A **44**, 5178 (1991).
[8] L. H. Yu *et al.*, Phys. Rev. Lett. **91**, 074801 (2003).
[9] R. Bonifacio *et al.*, Riv. Nuovo Cimento Soc. Ital. Fis. **13**, 1 (1990).
[10] R. Bonifacio *et al.*, Nucl. Instrum. Methods Phys. Res., Sect. A **296**, 358 (1990).
[11] D. A. Jaroszynski *et al.*, Phys. Rev. Lett. **78**, 1699 (1997).
[12] T. Watanabe *et al.*, Phys. Rev. Lett. **98**, 034802 (2007).
[13] M. E. Couprie *et al.*, in Proceedings of the EPAC'08 Conference, Genoa, Italy (JACOW, 2008), Vol. 1, p. 73.
[14] E. Allaria *et al.*, in Proceedings of the FEL Conference 2006, Berlin, Germany (JACOW, 2007), p. 166.
[15] C. Vaccarezza *et al.*, in Proceedings of the PAC'07 Conference, Albuquerque, New Mexico (JACOW, 2007), Vol. 1, p. 1001.
[16] W. B. Colson, Phys. Lett. A **59**, 187 (1976).
[17] G. Lambert *et al.*, Nature Phys. **4**, 296 (2008).
[18] L. Giannessi *et al.*, Nucl. Instrum. Methods Phys. Res., Sect. A **593**, 26 (2008).
[19] M. Labat *et al.*, Nucl. Instrum. Methods Phys. Res., Sect. A **593**, 132 (2008).
[20] A. Azima *et al.*, in Proceedings of the EPAC'08 Conference, Genoa, Italy (JACOW, 2008), Vol. 1, p. 127.
[21] R. Bonifacio *et al.*, Nucl. Instrum. Methods Phys. Res., Sect. A **239**, 29 (1985).
[22] S. Reiche *et al.*, Nucl. Instrum. Methods Phys. Res., Sect. A **593**, 45 (2008).
[23] A. E. Siegman, *Lasers* (University Science Books, Mill Valley, CA, 1986), p. 1171.
[24] R. Bonifacio *et al.*, Riv. Nuovo Cimento Soc. Ital. Fis. **13**, 1 (1990).